Ionic solids at high pressures and elevated temperatures: MgO (periclase)

N. L. Allan, M. Braithwaite, D. L. Cooper, W. C. Mackrodt, and S. C. Wright

Citation: The Journal of Chemical Physics **95**, 6792 (1991); doi: 10.1063/1.461517
View online: http://dx.doi.org/10.1063/1.461517
View Table of Contents: http://scitation.aip.org/content/aip/journal/jcp/95/9?ver=pdfcov
Published by the AIP Publishing

Ionic solids at high pressures and elevated temperatures: MgO (periclase)

N. L. Allan
School of Chemistry, University of Bristol, Cantocks Close, Bristol, BS8 1TS, England

M. Braithwaite
ICI Explosives Group Technical Centre, Ardeer Site, Stevenston, Ayrshire, KA20 3LN, Scotland

D. L. Cooper
Department of Chemistry, University of Liverpool, P. O. Box 147, Liverpool, L69 3BX, England

W. C. Mackrodt
ICI Chemicals and Polymers, P. O. Box 8, The Heath, Runcorn, Cheshire, WA7 4QD, England

S. C. Wright
Department of Chemistry, University of Liverpool, P. O. Box 147, Liverpool, L69 3BX, England

(Received 9 January 1991; accepted 9 July 1991)

An equation of state for MgO is calculated for conditions of high pressure and temperature using atomistic simulations within the quasiharmonic approximation with two-body potentials and a simple shell model. It is shown that experimental Hugoniot data can be reproduced accurately; other important properties are also examined including various quantities of geophysical interest. Results for the Helmholtz free energy and internal energy surfaces $A(V,T)$ and $U(V,T)$ are presented in parametrized form.

I. INTRODUCTION

Accurate equations of state for crystalline materials are very important in many applications involving high pressures and elevated temperatures. Such areas include geophysical studies of planetary cores, the behavior of shocked condensed matter, explosives technology, materials processing, and studies of nuclear fuels.

These equations of state allow comparisons of theoretical thermodynamic predictions and corresponding experimental data from disparate sources such as shock Hugoniot results and diamond anvil cell experiments. The resultant equations can, in principle, be used for estimation of thermodynamic properties for a particular condensed phase over a wide range of density and temperature.

MgO (periclase) is a "classic" ceramic material and it is also a dominant mineral phase of the Earth's lower mantle.[1] It is very important to be able to understand and where necessary predict the variation of the structural and physical properties of MgO with temperature and pressure.

MgO has been much studied both experimentally and theoretically.[2–4] The purpose of the current paper is to present results for thermodynamic properties, and corresponding derivatives, of MgO over extended ranges of density and temperature. Where appropriate, results are presented in parametrized form suitable for inclusion in modern chemical equilibrium, detonation, and finite element computer codes; these require the rapid evaluation of quantities such as Helmholtz free energy, pressure, and entropy.

The accuracy of our equation of state is tested by suitable comparisons with available shock Hugoniot and bulk modulus data. For face-centered-cubic (fcc) MgO, the transition to the body-centered-cubic (bcc) phase, common in other systems with the rock-salt structure, is believed to occur at very high pressures (considerably above 120 GPa), and so this phase change can be neglected in the calculations presented here.

Modern developments in generating potentials for ionic systems[5] to represent the non-Coulombic interactions between the ions means that it is now possible to consider theoretically, using atomistic simulation techniques, a more comprehensive range of binary oxide and halide systems than hitherto. Studies of further important systems, including several that undergo phase transitions under the conditions of interest, will be the subject of a forthcoming publication.

II. THEORETICAL ASPECTS

The theoretical methods employed here are broadly similar to those used previously for a wide range of studies of ceramic oxides at zero pressure.[6–8] The simulations are based on an ionic model with formal charges of $+2$ and -2 for the Mg^{2+} and O^{2-} ions, respectively. Two different sets of two-body potentials were used to represent the non-Coulombic interactions between the ions: nonempirical potentials, based on a modified electron-gas approximation[9] of the type suggested by Gordon and Kim,[10] and "empirical" potentials.[11] Electronic polarization effects, essential for the accurate representation of the phonon frequencies, were incorporated via the shell model first introduced by Dick and Overhauser.[12,13] The short-range interactions were taken to act between the massless shells and the shell charges and spring constants were fitted to the static and high-frequency dielectric constants. The empirical and nonempirical potentials used in this work were taken from the literature without alteration. Both the implementation and the success of these potentials in predicting properties such as elastic constants

 0021-9606/91/216792-08$03.00

and lattice energies at zero temperature and pressure have been described in detail previously.[8,9,11]

As discussed elsewhere,[5,6,14] the nonempirical and empirical potentials used in this work are very similar at separations that correspond to the equilibrium interionic distance at zero pressure and temperature. The form of all the potentials is shown in Fig. 1. The empirical and nonempirical Mg^{2+}/O^{2-} potentials are very similar over wide ranges of nuclear separations. However, the two O^{2-}/O^{2-} potentials differ considerably from one another at much shorter oxygen–oxygen separations, which could be sampled at high pressures. One purpose of the current work is to assess the sensitivity of the calculated properties of MgO at high pressure to the potentials employed. The differences between empirical and nonempirical potentials at short oxygen–oxygen distances has important consequences for simulations of defective lattices and surfaces.

The detailed implementation of the standard shell model[13,15] we have employed is discussed in detail by Sangster and Strauch.[16] We work within the well-established quasiharmonic approximation. At a sufficiently high temperature, for any pressure, the interionic separations are such that the quasiharmonic approximation breaks down. Such a failure leads to striking discontinuities in the variation with temperature of calculated properties such as the entropy or the expansion coefficient. Typically, such behavior is only observed when lattice separations appropriate to those near the melting point are sampled. Such volumes are not considered in the present work. Indeed, for any given temperature, higher pressures correspond to smaller volumes and so this problem is not encountered over the range of temperatures and pressures considered in this work.

A convenient starting point for the present calculations is the evaluation of the Helmholtz free energy A given by

$$A = U_{el} + k_B T \sum_{\mathbf{k}j} \left(\tfrac{1}{2}\beta_j(\mathbf{k}) + \ln\{1 - \exp[-\beta_j(\mathbf{k})]\}\right), \tag{1}$$

where

$$\beta_j(\mathbf{k}) = \frac{h\nu_j(\mathbf{k})}{k_B T}$$

and k_B is the Boltzmann constant. $\nu_j(\mathbf{k})$ are the normal mode frequencies for wave vector $\mathbf{k}$, determined from the eigenvalues of the appropriate dynamical matrix, and U_{el} is the potential energy of the lattice. Both U_{el} and $\nu_j(\mathbf{k})$ are functions of the volume, but not of the temperature. The first term in the summation $\frac{1}{2}k_B T\beta_j(\mathbf{k})$ is the zero-point vibrational energy. The summation over wave vectors $\mathbf{k}$ in Eq. (1) is taken to be over the Chadi–Cohen special points in the irreducible part of the Brillouin zone.[17]

Given the exact differential

$$dA = -S\,dT - p\,dV,$$

it is straightforward to obtain the entropy S and the pressure p by differentiation

$$S = -\left(\frac{\partial A}{\partial T}\right)_V \quad \text{and} \quad p = -\left(\frac{\partial A}{\partial V}\right)_T$$

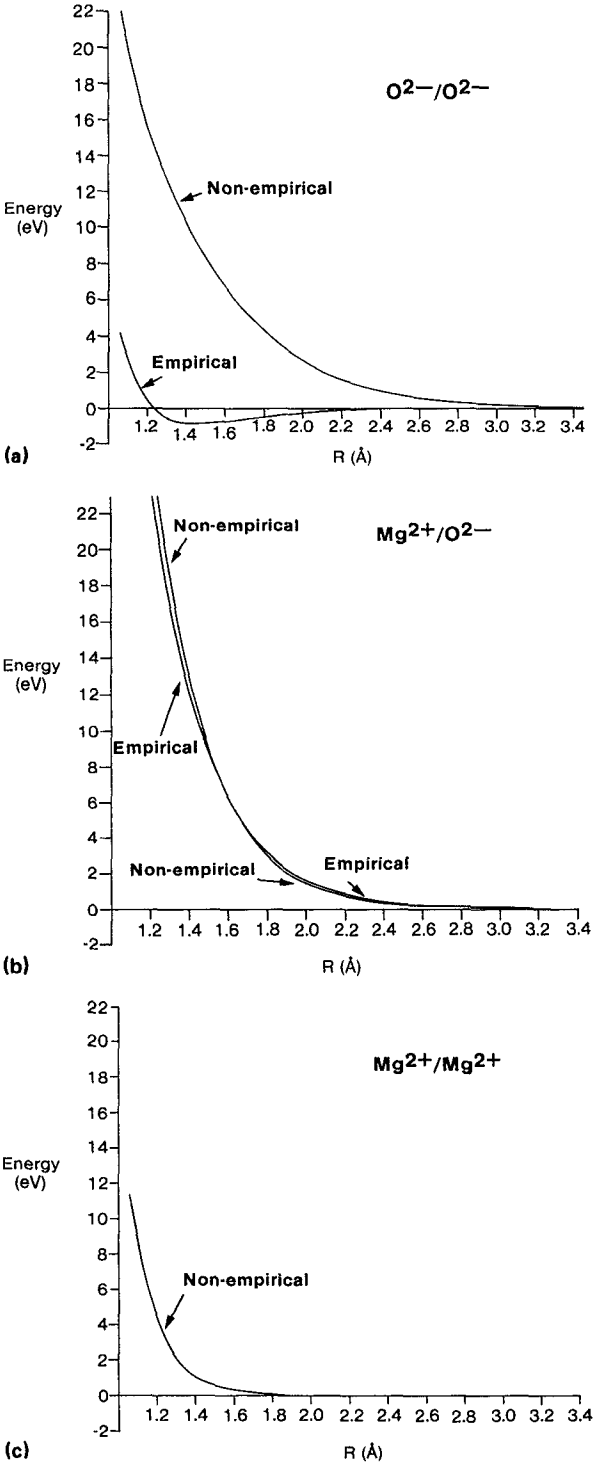

FIG. 1. The two-body potentials used in this work: (a) O^{2-}/O^{2-}; (b) Mg^{2+}/O^{2-}; (c) Mg^{2+}/Mg^{2+}. The empirical potentials take the form $V(R) = Ae^{-R/\rho} - C_6/R^6$ with $A = 22\,764.3$ eV, $\rho = 0.149$ Å, $C_6 = 20.37$ eV Å^6 for O^{2-}/O^{2-}, $A = 1346.6$ eV, $\rho = 0.2984$ Å, $C_6 = 0$ for Mg^{2+}/O^{2-}, and $A = C_6 = 0$ for Mg^{2+}/Mg^{2+}.

The calculated Helmholtz free energies $A(V,T)$ were fitted to an analytic function of volume and temperature $A_{MgO}(V,T)$, which will be described later. The calculated internal energies $U(V,T)$ were fitted with an analogous analytic function $U_{MgO}(V,T)$. Pressures were obtained by ana-

lytic differentiation of $A_{MgO}(V,T)$, but differences from the values obtained by numerical differentiation of $A(V,T)$ were negligible over the range of V and T considered.

We also present a Hugoniot trajectory determined from our calculated equation of state. The Rankine–Hugoniot relation takes the form

$$U_f - U_i = \tfrac{1}{2}(p_f + p_i)(V_i - V_f), \tag{2}$$

where the subscripts i and f label, respectively, the undisturbed solid and the solid behind the shock front. The temperature corresponding to p_f and V_f is the shock-front temperature. The experimental Hugoniot data[18,19] are obtained from measurements of shock-wave and particle velocities v_s and v_p. These last are given by

$$v_p = \left[\frac{2(U_f - U_i)}{V_i \rho_i}\right]^{1/2} \tag{3}$$

and

$$v_s = \frac{p_f}{\rho_i v_p}, \tag{4}$$

where ρ_i is the initial density. The calculation of Hugoniot equations of state is normally considered to be a severe test of interionic potentials.[20]

Our primary interest in this study is in the behavior of MgO at elevated temperatures and pressures. At low temperatures, the accurate evaluation of the entropy requires a more elaborate integration over the Brillouin zone than is employed here. In addition, as is discussed later, properties related to the compressibility are not reproduced well at zero pressure. This arises because $(\partial^2 A/\partial V^2)_T$ is not sufficiently accurate near the minimum value of A for a given V.

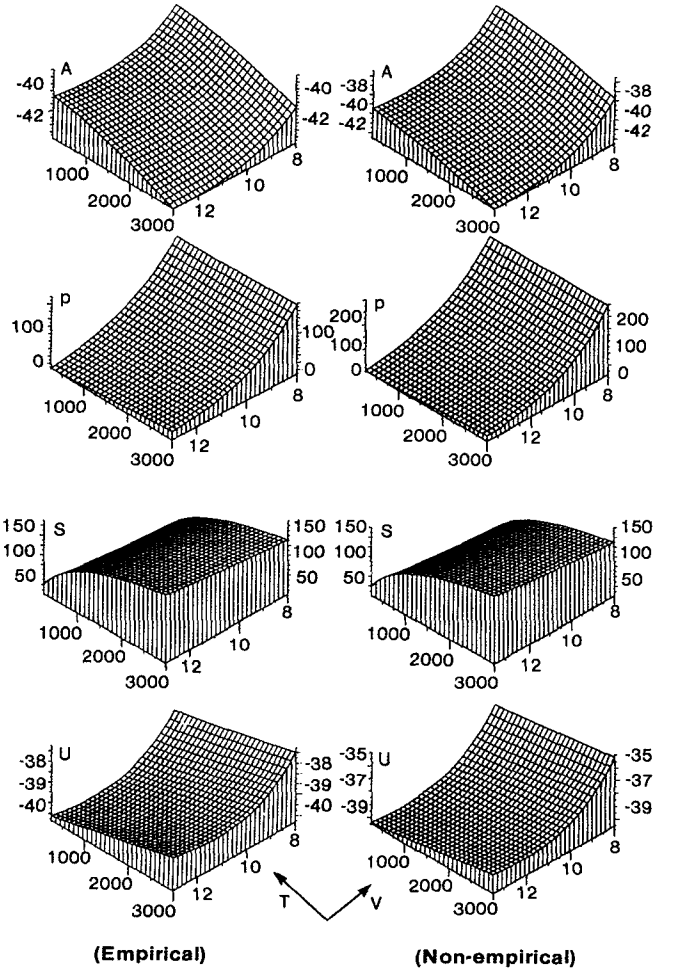

FIG. 2. $A(V,T)$, $p(V,T)$, $S(V,T)$, and $U(V,T)$ surfaces calculated for MgO using empirical and nonempirical potentials. A and U are in eV, p in GPa, S in J mol^{-1} K^{-1}, T in K, V in cm^3 mol^{-1}.

III. RESULTS

Figure 2 shows the calculated $A(V,T)$, $p(V,T)$, $S(V,T)$, and $U(V,T)$ surfaces over a range of temperature from 300 to 4500 K for both nonempirical and empirical potentials. The $p(V,T)$ surfaces were obtained by differentiation of the corresponding $A(V,T)$ surfaces with respect to V.

Anderson and Zou[2] have calculated a very comprehensive set of thermodynamic quantities for MgO using a scheme based on the product of the experimental values of the expansion coefficient and the isothermal bulk modulus, and the Birch–Murnaghan equation of state of the third degree.[21] The agreement with our calculated values is very satisfactory. For example, we present in Fig. 3 a comparison for $G(T,p)$ and $S(T,p)$, over a range of pressures, between our results and those tabulated in Ref. 2. The agreement between the two sets of values of $S(T,p)$ is particularly striking.

Figure 4(a) shows the variation of the molar volume with pressure at 300 K. The calculated curves for both empirical and nonempirical potentials run almost exactly parallel to the experimental data of Mao and Bell[22] (except for the value at zero pressure). Accordingly, the variation of V–V' with p is shown in Fig. 4(b), where values of V' have been chosen according to a least-squares criterion. The actual values of V' used to construct Fig. 4(b) are 0.40 and 1.39 cm^3/mol for the empirical and nonempirical potentials, respectively.

It is important to emphasize that the two-body potentials used in the present work were taken directly from the literature, without any attempt to modify them so as to reproduce the correct lattice constant at 300 K and zero pressure. The parameters in the empirical potential were in fact obtained in such a way that the lattice constant at zero temperature and zero pressure is reproduced when neglecting all terms except the static contribution to the lattice energy.[11] Furthermore, the nonempirical potentials were obtained from a quantum-mechanical procedure with no fitting to lattice constants at any temperature or pressure.[9] In that our aim is to establish a simple general procedure, which is readily applicable to a large number of systems, it seems much more appropriate to use potentials from standard compilations than to modify potentials so as to better reproduce lattice constants under particular conditions.

It is clear from Fig. 4(b) and from the experimental value of the molar volume at 300 K and zero pressure

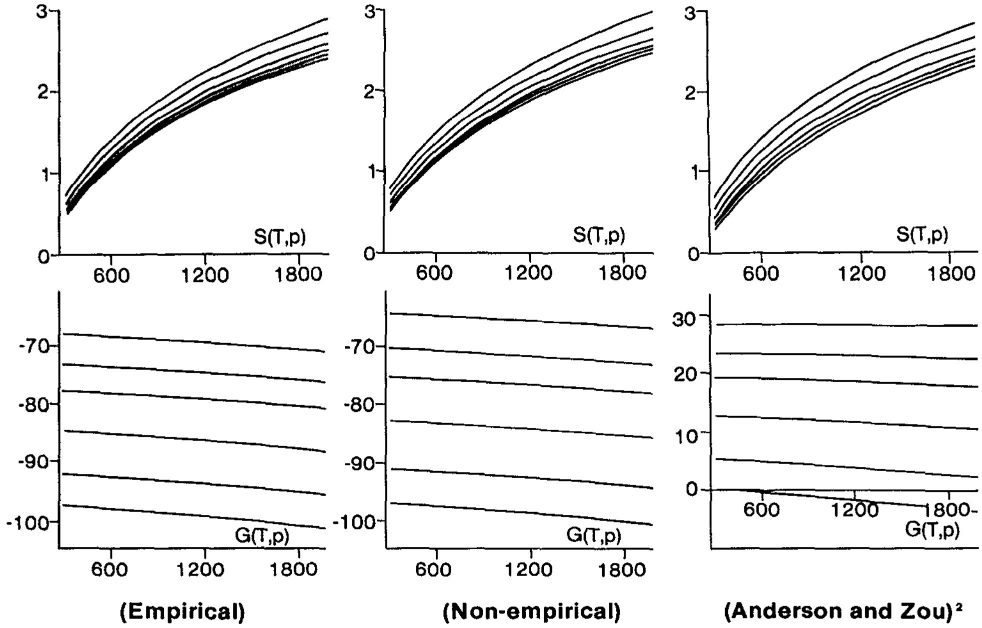

FIG. 3. Isobaric plots of the entropy S (in J g^{-1} K^{-1}) and Gibbs free energy G (in kJ g^{-1}) vs temperature. Results from calculations using empirical and nonempirical potentials are shown, as well as values estimated by Anderson and Zou (AZ) (Ref. 2). In each $S(T,p)$ frame, the pressures of each isobar (from top to bottom) are 0, 20, 50, 80, 100, and 125 GPa. In each $G(T,p)$ frame, the pressures (from top to bottom) are 125, 100, 80, 50, 20, and 0 GPa. Note that AZ have set $G(T=0, p=0)=0$.

($V=11.245$ cm^3/mol) that the present calculations underestimate the bulk compressibility at very low pressures. This problem has also been noted in zero pressure static calculations.[9] However, at pressures larger than $\approx$20 GPa, our calculated compressibilities are in much better agreement with experiment. Since the purpose of this work is to develop and test equations of state for elevated pressures (and temperatures), attempts to improve the low pressure behavior do not seem particularly worthwhile.

Comparisons of calculated and experimental Hugoniot data, in both p–V and v_s–v_p forms, are shown in Figs. 5(a) and 5(b). The agreement between theory and experiment is satisfactory in the sense that the calculated curves closely parallel the experimental results. The agreement can be improved by shifting v_f in exactly the same way as described above in the context of the p–V isotherm at 300K. For example, we show in Fig. 5(c) the analog of Fig. 5(a) when V_f in the Rankine–Hugoniot relation (2) is replaced by $V_f - V'$, with values of V' identical to those used for the p–V isotherm.

The thermal Grüneisen parameter γ is given by

$$\gamma = \sum_{\mathbf{k},j} \gamma_j(\mathbf{k}) C_j(\mathbf{k}) \Big/ \sum_{\mathbf{k},j} C_j(\mathbf{k}), \tag{5}$$

where $C_j(\mathbf{k})$ is the contribution of the mode $\nu_j(\mathbf{k})$ to the specific heat and $\gamma_j(\mathbf{k})$ are the so-called mode Grüneisen parameters

$$\gamma_j(\mathbf{k}) = \frac{d \ln[\nu_j(\mathbf{k})]}{d \ln(V)}. \tag{6}$$

In keeping with the experimental findings, our calculated value of γ is not very sensitive to temperature. The variation of γ with pressure at 800 and 1500 K is shown in Fig. 6. The reduction in γ with increasing pressure is much more marked than that calculated recently by Agnon and Bukowinski.[23]

A common assumption,[24] often used in the reduction of experimental data, is that the logarithmic isothermal volume derivative of the Grüneisen parameter

$$q = [\partial \ln(\gamma) / \partial \ln(V)]_T \tag{7}$$

can be taken to be constant at moderate compressions. Accordingly, we have also computed the variation of q with pressure at several temperatures. For pressures above $\approx$20 GPa, where our equation of state should be most accurate, we find that q is not very dependent on pressure. Whereas Agnon and Bukowinski calculate values of q which are smaller than γ at all pressures, our values of q are larger than those of γ, in keeping with the existing experimental data.

Anderson[25] has deduced from seismic observations of the acoustic behavior of the oxide mantle that the quantity $[\partial \ln(v_s)/\partial \ln(v_p)]_p$ lies in the range 2–2.5. Neglecting various changes such as melting and neglecting variation of composition, this finding suggests that the Anderson–Grüneisen parameter δ_s should decrease significantly at elevated pressures. Accordingly, we have evaluated δ_s using the relation

$$\delta_s = -(\alpha K_S)^{-1} (\partial K_S / \partial T)_p, \tag{8}$$

where K_S is the isoentropic bulk modulus. K_S is related to the isothermal bulk modulus K_T by $K_S/K_T = (1 + \alpha\gamma T)$. We find values for δ_s in the range 3–5, in keeping with laboratory studies of mantle minerals. Our calculated Anderson–Grüneisen parameters do not decrease markedly at large pressures. This is consistent with the conclusions of Reynard and Price,[26] but contrary to the results of Agnon and Bukowinski.[23] Partial melting has been invoked as one

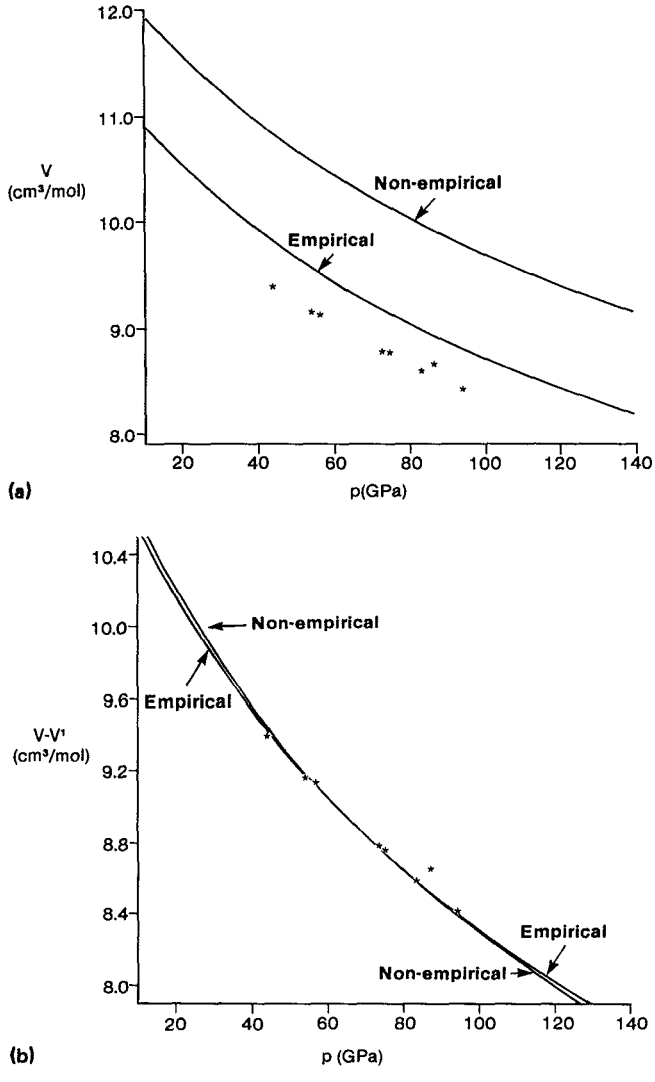

FIG. 4. p–V isotherms at 300 K for both empirical and nonempirical potentials. The experimental values of Mao and Bell (Ref. 22) are marked with crosses. (a) Variation of the molar volume V (in $cm^3\ mol^{-1}$) with pressure p (in GPa). (b) Variation of V–V' with p, where V' is 0.40 $cm^3\ mol^{-1}$ for the empirical potentials and 1.39 $cm^3\ mol^{-1}$ for the nonempirical potentials, respectively.

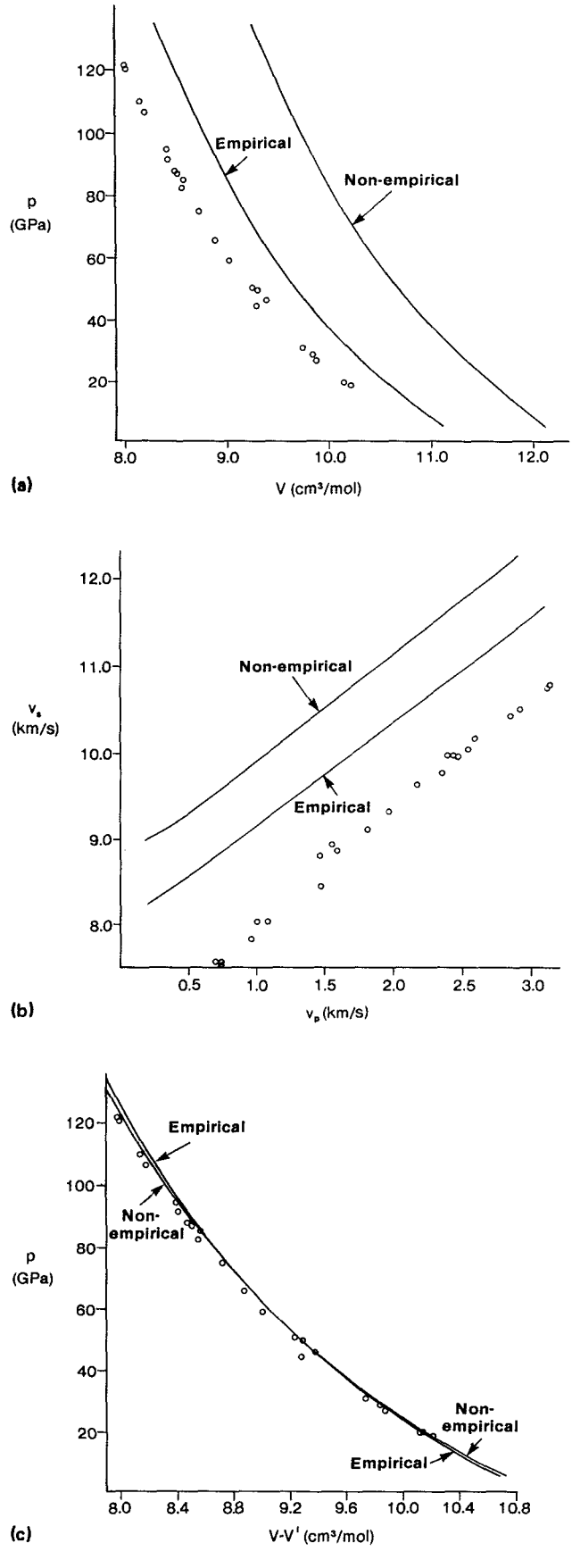

FIG. 5. Comparison of calculated Hugoniot data with experimental results from Ref. 18. (a) p (in GPa) vs V (in $cm^3\ mol^{-1}$); (b) v_s (in km s^{-1}) vs v_p (in km s^{-1}); (c) p vs V–V', with the same values of V' as in Fig. 4(b).

explanation of the lower mantle seismic data; the various possibilities have been discussed by Reynard and Price.

Another quantity of considerable interest is the temperature dependence of the "thermal pressure" $(\partial p/\partial T)_V$, which is equal to αK_T, the product of the thermal expansion coefficient and the isothermal bulk modulus. Geophysical models typically assume that αK_T is independent of volume and temperature for mantle minerals.[27–29] The variation with temperature of αK_T at pressures of 20 and of 100 GPa is illustrated in Fig. 7 both for nonempirical and empirical potentials. Also shown are the zero-pressure values of Anderson and Zou,[2] which were calculated directly from experimental data. At both of the pressures we have considered, we find at high temperatures that αK_T is only weakly dependent on temperature and that the variation is slightly

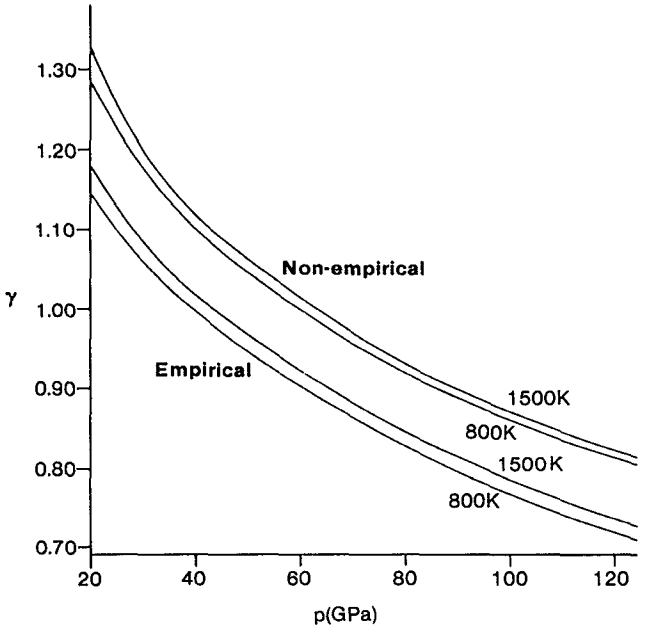

FIG. 6. Variation with pressure of the thermal Grüneisen parameter γ at 800 and 1500 K.

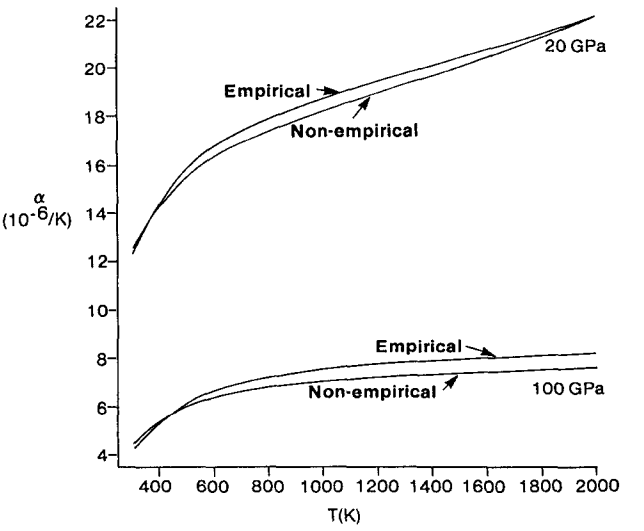

FIG. 8. Variation with temperature of the thermal expansion coefficient α (in 10^{-6} K^{-1}). Calculated results for empirical and nonempirical potentials are shown for pressures of 20 and 100 GPa.

less marked than that reported by Anderson and Zou[2] for zero-pressure data.

The validity of models such as those of Anderson and Zou[2] and of Vinet *et al.*[29] rely in part on a weak volume dependence for αK_T. Our calculations support this assumption. This is particularly reassuring for the geophysical models, because the original proposals made by Birch[27] were based only on results for alkali metals up to 3 GPa.

Over the pressure range considered in this paper, the value of the thermal expansion coefficient α (see Fig. 8) decreases by a factor in the range 4–6. We find that α is approximately proportional to V^t at 300 K, where $t \approx 6$, in good agreement with the value of $t = 6.5$ obtained by Chopelas[30] from the measurement of vibronic bands in the fluorescence spectrum of Cr^{3+}-doped MgO under pressures of up to 200 kbar. This contrasts with the value $t = 3$ used by Anderson.[25] Other materials exhibit similar behavior in that α decreases by approximately an order of magnitude. This variation of α has important consequences for lower mantle topography[31] and for estimates of the lower mantle density.[32]

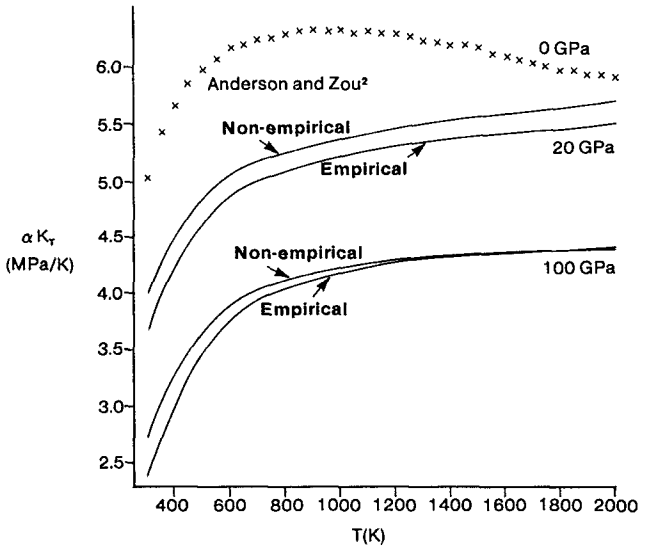

FIG. 7. Variation with temperature of the thermal pressure αK_T (in MPa K^{-1}). Calculated results for empirical and nonempirical potentials are shown for pressures of 20 and 100 GPa. The experimental zero-pressure values from Ref. 2 are denoted by crosses.

The calculated isothermal transition at 300 K to the body-centered phase (CsCl structure) is predicted to occur at very high pressures, well above 120 GPa, and this is in agreement with previous work.[33] Analogous conclusions are reached for the isoentropic phase change by comparing the enthalpies of the two phases as a function of pressure. This is the justification for the neglect of the phase change for the range of temperatures and pressures considered in the current work. Our findings support the conclusion of Vassiliou and Ahrens[19] that the fcc–bcc phase transition is unlikely to be important in the lower mantle, where pressures are less than ≈ 130 GPa.

Finally, it is convenient for many applications to express $A(V,T)$ in a parametrized form and so an appropriate fitting procedure was used as follows: For each value of V, $A(V,T)$ was first fitted to quadratics in T according to

$$A(V,T) = a(V)T^2 + b(V)T + c(V).$$

The volume-dependent quadratic coefficients $a(V)$, $b(V)$, and $c(V)$ were then each fitted as cubics in V. Analytic differentiation of the resulting expression with respect to V gave pressures in fair agreement with the values obtained by numerical differentiation of the calculated Helmholtz free energies. The residual was found to be essentially indepen-

dent of temperature and to have a quartic dependence on V. Accordingly, a further quintic polynomial in V was fitted to the residuals in the analytic representation of $A(V,T_{\rm mid})$, where $T_{\rm mid}$ is the average of the lowest and highest temperatures considered. After inclusion of this quintic in V, the residuals in the fit of $A(V,T)$ were found to be very small and to be essentially independent of the volume. These minor differences could be reduced still further by fitting a quartic polynomial in T to the residuals in the analytic representation of $A(V_{\rm mid},T)$, where $V_{\rm mid}$ is the average of the smallest and largest volumes considered. The final analytic expression $A_{\rm MgO}(V,T)$ therefore takes the form

$$A_{\rm MgO}(V,T)=\left(\sum_{i=0}^{3}\sum_{j=0}^{2}c_{ij}V^iT^j\right)+c_{04}T^4+c_{03}T^3+c_{50}V^5+c_{40}V^4. \quad (9)$$

The $S_{\rm MgO}(V,T)$ surface, obtained by analytic differentiation of $A_{\rm MgO}(V,T)$ with respect to T, is in remarkable agreement with the one shown in Fig. 2. In principle, values of $U(V,T)$ can be obtained directly from $A_{\rm MgO}+T\times S_{\rm MgO}$, but we found that slightly better agreement with the surface shown in Fig. 2 could be obtained using a separate fit. The expression used to fit the calculated values of $U(V,T)$ takes the same analytic form as for $A(V,T)$ and the 16 independent parameters were determined using a strategy analogous to the one just described.

The fitted values of the c_{ij} parameters appearing in $A_{\rm MgO}(V,T)$ and $U_{\rm MgO}(V,T)$ are collected in Table I. It should be emphasized that the range of validity of these functional forms is limited to the range of volumes and temperatures shown in Fig. 2. These functional forms reproduce fairly well the calculated $A(V,T)$, $p(V,T)$, $S(V,T)$, and $U(V,T)$ surfaces, but higher derivatives cannot be expected to be reliable. More accurate fits of the calculated surfaces are provided by interpolating rational functions expressed in continued fraction form and these were used to calculate all of the quantities shown in Figs. 3 and 5–8, as well as those discussed in the text. Further details are available from the authors on request.

IV. CONCLUSIONS

We have used the quasiharmonic approximation, together with shell-model lattice dynamics and standard two-body interionic potentials, to calculate a considerable number of thermodynamic quantities for MgO (periclase) over a wide range of temperatures and pressures. Under the conditions we have considered, the internuclear distances are such that anharmonic effects are presumably suppressed.

Our procedure appears to give good values for numerous properties, including various quantities of geophysical interest. Parametrized forms of $A(V,T)$ and $U(V,T)$ are also presented; reliable $p(V,T)$ and $S(V,T)$ surfaces can be derived from the Helmholtz free energy by taking the appropriate derivatives.

Using two-body potentials, we obtain poor values for the compressibility at the smallest pressures because such potentials cannot account for the Cauchy violation. This problem could be resolved by using an appropriate three- or higher-body potential. Nevertheless, the success of the traditional simple shell model at higher pressures (and temperatures) is striking. Studies of the behavior of MgO and similar solids using constant-pressure molecular dynamics (see, e.g., Ref. 3) would be very worthwhile for comparative purposes.

Over the range of temperatures and pressures considered here, the results from the empirical and nonempirical potentials are similar except that the volumes predicted by the nonempirical potential are too large. Preliminary results for even higher pressures indicate that the calculated com-

TABLE I. Fitted values of the c_{ij} parameters appearing in $A_{\rm MgO}(V,T)$ and $U_{\rm MgO}(V,T)$. c_{ij} is the coefficient of V^iT^j, where V is in cm^3 mol^{-1}, T is in K, and $A_{\rm MgO}$ and $U_{\rm MgO}$ are in eV (as in Fig. 2).

	Empirical potentials		Nonempirical potentials	
	$A_{\rm MgO}$	$U_{\rm MgO}$	$A_{\rm MgO}$	$U_{\rm MgO}$
c_{32}	−3.824 64E−12	−4.263 01E−13	−1.952 01E−12	−7.784 38E−14
c_{22}	2.267 20E−10	1.620 62E−10	1.357 92E−10	1.023 34E−10
c_{12}	−4.718 67E−09	−5.427 97E−09	−3.358 40E−09	−4.152 77E−09
c_{02}	−5.810 94E−07	2.596 00E−07	−5.845 31E−07	2.557 69E−07
c_{31}	−5.331 46E−07	9.833 32E−09	−5.123 47E−07	4.613 47E−09
c_{21}	1.251 61E−05	−1.037 38E−06	1.284 09E−05	−6.409 93E−07
c_{11}	−1.356 51E−04	2.844 75E−05	−1.437 32E−04	2.124 58E−05
c_{01}	7.387 78E−04	6.127 61E−05	7.841 31E−04	9.361 37E−05
c_{30}	−5.353 95E−01	−4.910 33E−01	−7.353 46E−01	−7.045 17E−01
c_{20}	6.806 93E+00	6.408 81E+00	9.615 42E+00	9.336 61E+00
c_{10}	−4.489 17E+01	−4.317 10E+01	−6.514 34E+01	−6.393 85E+01
c_{00}	8.137 02E+01	7.852 78E+01	1.422 55E+02	1.402 83E+02
c_{04}	−1.517 62E−14	1.001 32E−14	−1.505 46E−14	1.015 60E−14
c_{03}	1.434 38E−10	−7.885 05E−11	1.424 61E−10	−7.992 11E−11
c_{50}	−3.641 86E−04	−3.131 10E−04	−4.671 51E−04	−4.326 56E−04
c_{40}	2.180 35E−02	1.939 71E−02	2.899 39E−02	2.734 23E−02

pressibility for $p > 200$ GPa is smaller for the nonempirical potential than for the empirical potential. This presumably reflects the different O^{2-}/O^{2-} potentials, in that the nonempirical potential is considerably more repulsive at short separations. However, over the range of temperature and pressures considered here, both sets of potentials give very similar results. The quantities we have calculated are evidently rather insensitive to the form of the O^{2-}/O^{2-} potential. The two sets of potentials do give different results for the volume dependence and it is clear from Figs. 4 and 5 that the empirical set is to be preferred.

In future work, we shall report analogous studies of other important rocksalt oxides and also various fluorides and chlorides. Phase changes occur for many of these systems within the range of temperatures and pressures of interest to us and these provide further severe tests of our simple model.

[1] R. Jeanloz and A. B. Thompson, Rev. Geophys. Space Phys. **21**, 51 (1983).
[2] O. L. Anderson and K. Zou, J. Phys. Chem. Ref. Data **19**, 69 (1990), and references therein.
[3] M. M. Matsui, J. Chem. Phys. **91**, 489 (1989).
[4] L. L. Boyer, Phys. Rev. B **27**, 1271 (1983).
[5] N. L. Allan, D. L. Cooper, and W. C. Mackrodt, Mol. Simulat. **4**, 269 (1990).
[6] W. C. Mackrodt, in *Computer Simulation of Solids*, edited by C. R. A. Catlow and W. C. Mackrodt (Springer, Berlin, 1982).
[7] W. C. Mackrodt, Solid State Ion. **12**, 175 (1984).
[8] N. L. Allan, W. C. Mackrodt, and M. Leslie, Adv. Ceram. **23**, 257 (1987).
[9] W. C. Mackrodt and R. F. Stewart, J. Phys. C **12**, 431 (1979).
[10] R. G. Gordon and Y. S. Kim, J. Chem. Phys. **56**, 3122 (1972).
[11] M. J. L. Sangster and A. M. Stoneham, Philos. Mag. B **52**, 717 (1985).
[12] B. G. Dick and A. W. Overhauser, Phys. Rev. **112**, 90 (1958).
[13] W. Cochran, Crit. Rev. Solid State Sci. **2**, 1 (1977).
[14] J. Kendrick and W. C. Mackrodt, Solid State Ion. **8**, 247 (1983).
[15] M. J. L. Sangster and A. R. Q. Hussain, Phys. Status Solidi B **131**, 119 (1985).
[16] M. J. L. Sangster and D. Strauch, J. Phys. Chem. Solids **51**, 609 (1990).
[17] D. J. Chadi and M. L. Cohen, Phys. Rev. B **8**, 5747 (1973).
[18] *LASL Shock Hugoniot Data*, edited by S. P. Marsh (University of California, Berkeley, 1980).
[19] M. S. Vassiliou and T. J. Ahrens, Geophys. Res. Lett. **8**, 729 (1981).
[20] J. H. Harding and A. M. Stoneham, J. Phys. C **17**, 1179 (1984).
[21] F. Birch, J. Appl. Phys. **9**, 279 (1938).
[22] H. K. Mao and P. M. Bell, J. Geophys. Res. **84**, 4533 (1979).
[23] A. Agnon and M. S. T. Bukowinski, Phys. Rev. B **41**, 7755 (1990).
[24] R. W. Roberts and R. Ruppin, Phys. Rev. B **4**, 2041 (1971).
[25] D. L. Anderson, Phys. Earth Planet Int. **45**, 307 (1987).
[26] B. Reynard and G. D. Price, Geophys. Res. Lett. **17**, 689 (1990).
[27] F. Birch, J. Geophys. Res. **57**, 227 (1952).
[28] O. L. Anderson, J. Geodyn. **1**, 185 (1984).
[29] P. Vinet, J. R. Smith, J. Ferrante, and J. H. Rose, Phys. Rev. B **35**, 1945 (1987).
[30] A. Chopelas, Phys. Chem. Minerals **17**, 142 (1990).
[31] U.Hansen and D. A. Yuen, Geophys. Res. Lett. **16**, 629 (1989).
[32] A. Chopelas and R. Boelner, Geophys. Res. Lett. **16**, 1347 (1989).
[33] See, e.g., A. J. Cohen and R. G. Gordon, Phys. Rev. B **14**, 4593 (1976).